

## Field emission properties of expanded graphite composite

**P.S. Alegaonkar, J.H. Park, S. Y. Jeon, J. H. Shin, A. S. Berdinsky  
and J. B. Yoo**

**Center for Nanotubes and Nanostructured Composites,  
Sungkyunkwan University, Suwon, 440-746, Korea  
TEL: 82-31-299-4745, email: [prashant@skku.edu](mailto:prashant@skku.edu)**

**Keywords: Expanded graphite. field emission properties. characterizations**

### Abstract

*Field emission properties of expanded graphite composite have been studied. Composite has been synthesized via shear mixing expanded graphite in  $\alpha$ -terpineol and ethyl cellulose. Field emission properties, of screen printed composite has been measured at a static applied electric field. The details of the analysis have been presented.*

### 1. Introduction

Field emission (FE) is a quantum mechanical phenomenon in which the kinetic energy of the electrons in the direction of applied electric field is essentially responsible for electron tunneling into the vacuum [1]. For metals and semiconductors, FE could be observed in electric field regime of 10–100 V/ $\mu$ m which is typically two orders of magnitude high as compared to the FE from carbon nanotubes [2]. In recent years, FE studies on graphitic carbon have become important issue from the point of view of technological applications as well as fundamental sciences. Graphene is a two-dimensional monolayer of hexagonally arranged carbon and bunch of such sheets is termed as graphite which could serve as a source for the FE. In such systems, FE mainly occurs via edges and bends (folding edges), however, the current density could be influenced by the edge dangling or  $\sigma$  bond states, condition of edge termination as well as their geometry (armchair or zigzag), local band structure of the bend and orientation of the graphene sheets with respect to the applied electric field.

A considerable amount of work related to the FE characteristics of the graphite [3] has been carried out. The nanostructured graphite of sheet thickness  $\sim$  10–50 nm, grown by CVD synthesis, have shown magnitude of turn-on-field  $\sim$  5 V- $\mu$ m<sup>-1</sup> and field enhancement factor,  $\gamma$ , in the range of 50–500 [4].

Free standing graphite sheets, synthesized by rf plasma enhanced CVD technique, of layer thickness  $\sim$  1 nm have shown turn-on-field  $\sim$  4.7 V- $\mu$ m<sup>-1</sup> at a threshold of 10  $\mu$ A-cm<sup>-2</sup> [5]. In another study, nano carbon films, synthesized by CVD technique, of layer thickness 2 nm–20  $\mu$ m have shown turn-on-field  $\sim$  10 V- $\mu$ m<sup>-1</sup> with corresponding field enhancement factor,  $\gamma$ , 500 [6]. In most cases such studies were carried out on as-grown graphitic films of layer thickness in the range of a few hundred nm to a few  $\mu$ m. In general, not much attention has been paid to FE studies of expanded graphite, synthesized via composite approach which is scalable for vacuum microelectronics and other applications. From the point of view of technological applications, it is of interest to explore FE parameters of expanded graphite composite, in order to obtain significant advantages in terms of turn-on-field and enhancement factor, without degrading the emission stability, significantly. In this contribution, we report that the threshold-turn-on field for a expanded graphite (EG) composite, could be obtained upto  $\sim$  8.02 V/ $\mu$ m with a mean field enhancement factor,  $\gamma_m$ , 700 $\pm$ 20 and geometric field emission area  $\sim$  10<sup>-14</sup>/cm<sup>2</sup>. The field emission properties have been studied at a static applied electric field.

### 2. Experimental

The readily available expanded graphite (EG)  $\sim$  0.5 mg was mixed with about 9.5 gm  $\alpha$ -terpineol (C<sub>10</sub>H<sub>18</sub>O, (R)-2-(4-Methyl-3-cyclohexenyl)-2-propenol) and subjected to the ultrasonication process for 12 h. Furthermore, the solution is mixed with ethyl cellulose and subjected to premixing for a period of 30 min. In addition to sonication, adequate shear stresses have been applied so that the graphene sheets untangle and disperse uniformly in the ethyl cellulose matrix. The mixture was employed to the calendering

process, for a residence time of ~ 15 min, by utilizing a commercially available laboratory scale three roll miller. The intense shear mixing occurred between the narrow gap of the rolls as well as the mismatch in angular velocity ( $\omega_3 = 3\omega_2 = 9\omega_1$ ) of the adjacent rolls due to compressive impact as well as shear stress [7]. The mill setting has been controlled electronically and the viscosity of the material was monitored during the calendering process.

The collected composite employed to the screen printing process to develop the cathode layers. The porous stencil diaphragm of area  $1 \times 1 \text{ cm}^2$  was placed on top of an Indium Tin Oxide (ITO) coated glass substrate. The composite was placed on the screen, and a squeegee (rubber blade) pushed to-and-fro for 3–4 times so that the composite uniformly entered into the screen openings and deposited onto the ITO coated glass. These cathodes were dried in the oven for ~ 30 min at  $90^\circ\text{C}$  and subjected to the annealing process at  $450^\circ\text{C}$  for about 10 min under nitrogen ambient, to remove the volatile organic components from the cathode. A large number of cathode layers have been fabricated. Following this, the tape activation treatment has been carried out [8] which selectively removed the mechanically weak over layer graphene sheets and oriented transverse sheets predominantly so that the basal planes protrude perpendicular to the surface.

The surface morphology of the cathode layers were examined by field emission scanning electron microscope (FESEM, JEOL, 30 kV).

Field emission measurements have been carried out at a static applied electric field, in a diode type configuration, at a base pressure of  $10^{-7}$  Torr. Super used steel (SUS) was used as an anode to collect the electrons. The inter-electrode distance was kept constant ~ 200  $\mu\text{m}$ . The static field was varied from 0.5 V/ $\mu\text{m}$  to 12 V/ $\mu\text{m}$ .

### 3. Results and discussion

Fig. 1 shows recorded FESEM micrograph for EG-composite cathode layers. The image has been taken in a cross-view. It can be seen that thin graphene sheets were lying on the ITO coated glass substrate.

Fig. 2 shows variations in the measured current density,  $J$ , as a function of applied electric field,  $E$ . The  $J$ - $E$  cycling has been carried out for about ~ 4 to 5 times, to obtain stable, reproducible characteristics. It can be seen that, over 0.5 to 7.0 V/ $\mu\text{m}$ , no significant variations in the FE current density has been observed, however, beyond 7.0 V/ $\mu\text{m}$  the

magnitude of current density changes dramatically

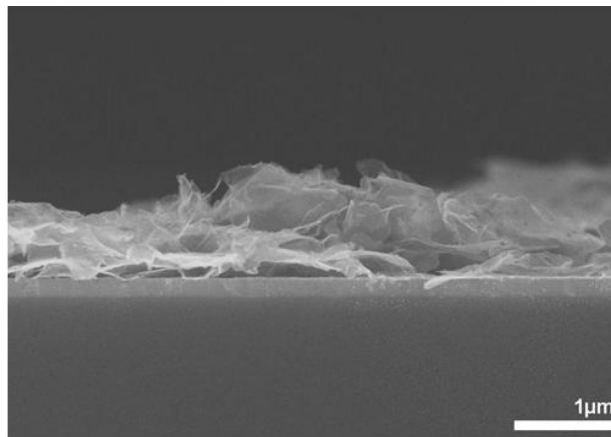


**Fig. 1. Recorded SEM image for EG composite.**

and observed to be strongly field dependent. The local density of FE current could be expressed by most commonly used Fowler–Nordheim equation in the voltage–based notion [9]:

$$J_{loc} = \frac{a \beta^2 V^2}{(t_F)^2 \Phi} \exp \left[ -\frac{v_F b \Phi^{3/2}}{\beta V} \right] \quad (1)$$

where  $V$  is the applied voltage,  $\beta$  is the conversion factor for the voltage–to–barrier–field (the field at the graphene edge that determines whether FE occurs),  $J_{loc}$  is the local current density,  $\Phi$  is the local work–function (~ 5 eV),  $a$  and  $b$  are universal constants (with  $a=1.541433 \times 10^{-6} \text{ A-eV-V}^{-2}$ ,  $b=6.830890 \times 10^3 \text{ eV}^{3/2}\text{-V-}\mu\text{m}^{-1}$ ), and  $v_F$  and  $t_F$  are mathematical functions known as the Nordheim functions, evaluated at the Fermi level. Tabulations of the special field emission elliptic functions  $v_F$  and  $t_F$  are given in the literature [10]. The value of  $v_F$  is typically ~ 0.70 for carbonaceous materials [11]. For a parallel–plate arrangement with the electrode separated by a gap of thickness  $d$ , we have  $\gamma = \beta d$ , with  $\beta = 1$  (for flat cathode). And the field enhancement factor,  $\gamma$ , is defined as “ $\gamma = \text{barrier-field} / \text{macroscopic field (applied field)}$ ”.

From the inset of Fig. 2 mean–field enhancement factor,  $\gamma_m$ , has been computed to be  $700 \pm 20$ . The corresponding area participating in the field emission process is found to be  $\sim 1.26 \times 10^{-14} / \text{cm}^2$ . The magnitude of threshold turn–on–field is found to be ~ 8.02 V/ $\mu\text{m}$  measured at a value of current density 10  $\mu\text{A} / \text{cm}^2$ .

In general, edge and bend, their geometry (arm chair, zigzag) and condition of termination are

responsible for the electron FE from the graphene sheets. At the edge and bend, the depletion of local

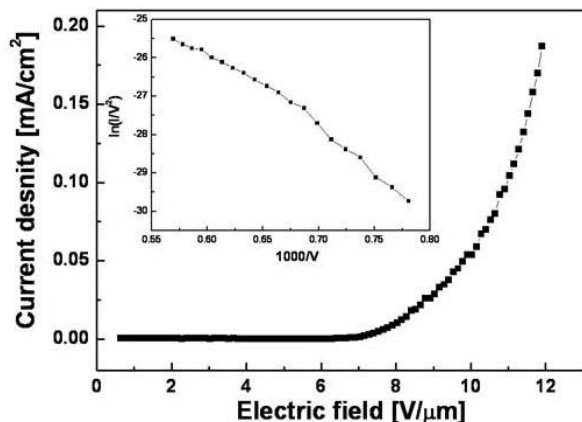


**Fig. 2. Variation in current density as a function of applied electric field (inset shows corresponding Fowler–Nordheim plot)**

barrier–field takes place as a result the current density enhances at lower magnitude of macroscopic–field. Moreover, the local direction of the edge with respect to the applied field and local electronic states on the edge are also responsible for the electron emission phenomena. The carbon atoms present on the edge of the basal plane have valance bonds in the dangling state. The electronic orbital of the dangling bond states tend to appear at the edge and protrude along the direction of the applied field, contributing in the electron FE phenomena. However, at the folding edge, the local band structure of graphene is changed due to the change in the degree of overlap of  $\pi$  electronic orbital of carbon atoms which in turn change the state of hybridization from  $sp^2$  to  $sp^3$ . The thickness of such folding edge is typically 1–2 nm which is 4–6 graphene layers (TEM not shown) and is transparent to tunneling electrons at a lower sub–threshold regime [12].

Thus, it is crucial to study field emission properties of expanded graphite composite. The result offers insight to use such nano–sheets for future electron emission device applications.

#### 4. Summary

Field emission properties of expanded graphite (EG) composite have been studied. Initially, readily available EG powder was admixed with  $\alpha$ -terpineol and ultrasonicated for about 12 h. The obtained solution was premixed for about 30 min with ethyl

cellulose. Following this, the mixture was subjected to the three roll milling (calendering process) for a period of 1 h. The composite has been screen printed on ITO coated glass substrate and after annealing subjected to field emission study. Measurements were carried out at a static applied field mode over a range of 0.5 to 12 V/ $\mu$ m. The threshold turn-on-field is observed to be  $\sim 8.02$  V/ $\mu$ m (at a magnitude of current density  $\sim 1$   $\mu$ A/ $\text{cm}^2$ ). The field enhancement factor is observed to be  $700 \pm 20$  with corresponding geometric area participating in the field emission process  $\sim 1.26 \times 10^{-14}$  /  $\text{cm}^2$ . The field emission occurred via edges and bends in the graphitic sheets; moreover, their geometry (arm chair, zigzag) and condition of termination also played curial role in the process.

#### 5. References

1. R. Gomer (ed.), Field Emission and Field Ionization, American Institute of Physics, p21 (1993).
2. W. A. de Heer, A. Chatelain and D. Ugarte, *Science*, **270**, 1179 (1995).
3. Y. Neo, H. Mimura, T. Matsumoto, *Appl. Phys. Letts.*, **88**, 073511 (2006).
4. A.N. Obraztsov, Al. A. Zakhidov, A.P. Volkov, D. A. Lyashenko, *Diamond and Related Materials*, **12** p446 (2003).
5. J.J. Wang, M.Y. Zhu, R. A. Outlaw, X. Zhao, D. M. Manos, B. B. Holloway, and V. P. Manna, *Appl. Phys. Letts.*, **85**[7], p1265 (2004).
- 6.
7. F. H. Gojnu, M. H. G. Wichmann, U. Kopke, B. Fiedler, K. Schulte, *Comps. Sci. and Technol.* **64**, p2363 (2004).
8. T.J. Vink, M. Cillies, J.C. Kriege, H.W.J.J. van de Laar, *Appl. Phys. Lett.*, **83** p3552 (2003).
9. R. H. Nordheim and L. W. Fowler, Proc. Roy. Soc. London, Ser. A **119**, p173 (1928).
10. A.S. Berdinsky, A. V. Shaporin, J. B. Yoo, J. H. Park, P. S. Alegaonkar, J. H. Han, G. H. Son, *Appl. Phys. A* **83**, p377 (2006).
11. J.M. Bonard, M. Croci, C. Klinke, F. Conus, I. Arfaoui, T. Stockli, A. Chatelain, *Phys. Rev. B* **67**, 085 412 (2003).
12. M. Araidai, Y. Nakamura, K. Watanabe, *Phys. Rev. B*, **70** p 245419 (2004).